tvst

Article

Optical Coherence Tomography Angiography in Extensive Macular Atrophy with Pseudodrusen-Like Appearance

Firuzeh Rajabian, Alessandro Arrigo, Alessandro Bordato, Stefano Mercuri, Francesco Bandello, and Maurizio Battaglia Parodi

Department of Ophthalmology, IRCCS Ospedale San Raffaele, University Vita-Salute, Milan, Italy

Correspondence: Firuzeh Rajabian, Department of Ophthalmology, IRCCS Ospedale San Raffaele, University Vita-Salute, via Olgettina 60, Milan 20132, Italy. e-mail: firuzeh.r@hotmail.co.uk

Received: April 10, 2019
Accepted: November 21, 2019
Published: February 7, 2020

Keywords: atrophic zone; EMAP; junctional zone; OCTA; optical coherence tomography; optical coherence tomography angiography; preserved zone; pseudodrusen-like; vessel density

Citation: Rajabian F, Arrigo A, Bordato A, Mercuri S, Bandello F, Battaglia Parodi M. Optical coherence tomography angiography in extensive macular atrophy with pseudodrusen-like appearance. Trans Vis Sci Tech. 2020;9(3):2, https://doi.org/10.1167/tvst.9.3.2

Purpose: Analyses of quantitative features of optical coherence tomography angiography (OCTA) in patients affected by extensive macular atrophy with pseudodrusen-like appearance (EMAP).

Methods: In a prospective case-control study, patients and age- and gender-matched healthy controls underwent complete ophthalmologic examination, including best corrected visual acuity (BCVA) measurement, biomicroscopy, fundus autofluorescence and spectral-domain optical coherence tomography (Spectralis HRA; Heidelberg Engineering GmbH, Heidelberg, Germany), and OCTA scans (DRI OCT Triton; Topcon Corporation, Tokyo, Japan). Vessel density in the superficial capillary plexus and deep capillary plexus (DCP) in the retina and choriocapillaris (CC) in the macula and optic disc were measured. The one-way analysis of variance test with Bonferroni correction was used for statistical assessments.

Results: Seven patients (14 eyes) and 10 controls were included in the study. The mean follow-up period was 3 ± 0.8 years. The mean BCVA of patients at baseline was 0.81 ± 0.43 (logarithm of the minimum angle of resolution [LogMAR]) and 1.05 ± 0.38 (LogMAR) at the final follow-up visit ($P = 0.006$). Quantitative analyses of retinal vessels revealed significant alterations, especially in the DCP and CC, in both atrophic and junctional zones in retina of EMAP patients compared with preserved zones and controls.

Conclusions: OCTA analysis characterized three different retinal regions in EMAP disease, corresponding to progressively deeper perfusion defects. Further investigations are warranted to explore the correlation between DCP changes and the extension of atrophy.

Translational Relevance: By expanding our pilot study, we may better define EMAP on the basis of vascular changes and eventually recognize earlier the direction of enlargement of atrophy by means of OCTA analyses.

Introduction

Extensive macular atrophy with pseudodrusen-like appearance (EMAP) is a rare macular disease characterized by bilateral and symmetrical atrophic lesions extending in a vertical axis, with or without foveal sparing. Pseudodrusen are typically present in the mid-periphery, whereas paving-stone degeneration is detectable in the far periphery.

Compared with other forms of macular diseases, in particular age-related macular degeneration (AMD), EMAP has distinctive features, including earlier age of onset in the fourth decade of life, a vertical axis of extension, faster deteriorating visual loss, night blindness, and photophobia.[1]

EMAP can be complicated with choroidal neovascularization (CNV), which is more aggressive and less responsive to antivascular endothelial growth factor treatment.[2,3]

The initial description of EMAP reported no association with other diseases, but there have been reports of EMAP cases with a family history of AMD or *ABCA4* gene variation.[3] Although previous studies

were dedicated to the structural optical coherence tomography (OCT) analysis of EMAP features, to date few studies have described retinal vascular changes in this retinal disease.[4] The aim of the present study is to describe the OCT angiography (OCTA) features in patients affected by EMAP.

Methods

The study design was a prospective, observational case series. All of the patients diagnosed with EMAP in our center from January 2015 to December 2017 were considered in the study, along with a group of healthy volunteers who were age- and gender-matched as control subjects. Written informed consent was obtained from all of the subjects included in the study. The procedures adhered to the tenets of the Declaration of Helsinki and were approved by the ethical committee of the institute.

All patients underwent a complete ophthalmological examination every 6 months, including best corrected visual acuity (BCVA) using standard ETDRS charts, slit-lamp examination, multimodal imaging with color photography, spectral-domain optical coherence tomography (SD-OCT) (Spectralis OCT, Heidelberg Engineering GmbH, Heidelberg, Germany), Spectralis fundus autofluorescence (FAF), and OCTA (DRI OCT Triton; Topcon Corporation, Tokyo, Japan). Central atrophy was assessed within 2000 µm according to the Consensus Definition for Atrophy Associated with AMD for complete retinal pigment epithelium (RPE) and outer retinal atrophy (cRORA), incomplete RPE and outer retinal atrophy (iRORA), complete outer retinal atrophy (cORA), and incomplete outer retinal atrophy (iORA)[5].

OCTA analysis included 9 × 9-mm acquisitions, centered on the fovea and on the center of the optic nerve head. Only high-quality images, assessed by the Topcon image quality index (≥60),[6] were considered. OCTA images were analyzed with the Topcon full spectrum amplitude decorrelation angiography algorithm. The superficial capillary plexus (SCP), deep capillary plexus (DCP), and choriocapillaris (CC) were segmented in the macula and the optic nerve head, and the radial peripapillary capillary (RPC) plexus segmentation was also obtained at the optic nerve head. Each automated segmentation was carefully reviewed and manually corrected if necessary. All reconstructions were exported in the .tiff format and loaded into ImageJ software (National Institutes of Health, Bethesda, MD; available at https://imagej.net/Welcome or http://rsb.info.nih.gov/ij/). Each image was binarized through a mean threshold, and vessel density (VD) was calculated on the final binarized images and compared to controls. Quantitative analysis was performed on the entire SCP, DCP, and CC reconstructions.

Furthermore, in order to detect vascular changes occurring along the patients' follow-up, we identified and divided OCTA reconstructions into three different areas with respect to the progression of the disease (zones A, B, and C). These regions were detected by baseline and final follow-up FAF images, with the region of definitively decreased FAF being considered to be atrophic (areas in which the level of darkness was close to 100% in reference to the optic nerve head/blood vessels). In particular, we defined zone A as the atrophic area visible at baseline, whereas zone C was where the non-atrophic retina was detected at the end of the follow-up. Zone B was the region surrounding zone A that became atrophic at the end of the follow-up. (Fig. 1)

For the separated OCTA quantitative analysis, we co-registered the FAF images to en face OCTA reconstructions by means of a rigid registration available in ImageJ. In particular, we adopted as reference points the optic nerve head and the large retinal vessels. In this way, it was possible to over-impose and to use the three different zones for the separate calculations of VD. All VD measures were compared to the overall VD quantification of healthy controls.

One-way analysis of variance statistical tests with Bonferroni correction were used to assess significant differences among the above-described measures, separately considering zone A versus zone B versus zone C versus controls. P values ≤ 0.05 were considered significant.

Results

Overall, a total of 7 EMAP patients (4 males, 3 females; 14 eyes) between the ages of 42 and 66 years (mean, 60.2 ± 10.52) were recruited. The mean follow-up period was 3 ± 0.8 years (range, 2.0–4.0). The mean BCVA of patients at baseline was 0.81 ± 0.43 (logarithm of the minimum angle of resolution [LogMAR]; ranging from 0.3 to 1.3 LogMAR) and was 1.05 ± 0.38 LogMAR at the final follow-up visit (P = 0.006).

The medical histories were insignificant except for one patient with a mutation in the *PITPNM3* gene. Anterior segment examination revealed no alteration. Fundus examination showed geographic atrophy of various sizes, from the posterior pole to the vascular arcades, with a larger vertical diameter. The lesions

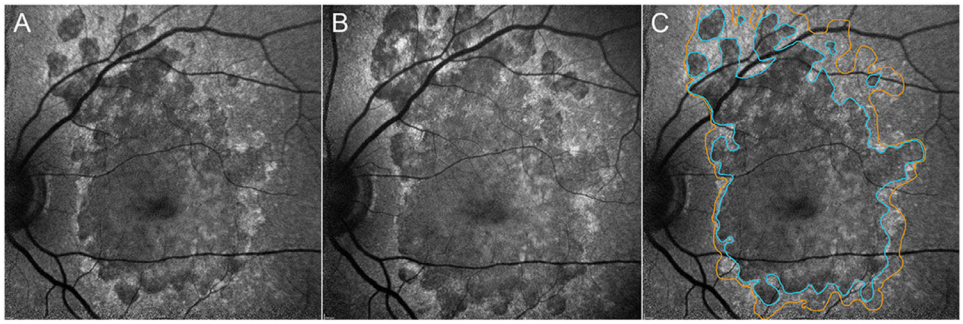

Figure 1. Fundus autofluorescence images at (A) baseline and at (B) final follow-up. (C) The area surrounded by a blue line is the atrophic zone visible at baseline (zone A), whereas the area outside the orange line is the non-atrophic retina detected at the end of the follow-up (zone C). Zone B is the area between the blue and orange lines in (C).

Table 1. Qualitative Analysis of SD-OCT Images in Vertical and Horizontal Axes and Division of Macular Involvement in Number of Eyes Affected by EMAP at Baseline and Final Visit

	Axis	cRORA	iRORA	cORA	iORA
Baseline	Vertical	3	9	0	2
	Horizontal	1	9	0	4
Final	Vertical	7	6	0	1
	Horizontal	5	6	0	3

turned out to be symmetrical in both eyes. In two patients, the atrophy progressed to the peripapillary and nasal retina during the follow-up period. All of the patients showed pseudodrusen surrounding the atrophy. Peripheral paving-stone degeneration was visible in all eyes. No eye developed CNV over the follow-up. Multimodal imaging features of EMAP are shown in Figure 2.

On FAF imaging, the atrophic areas appeared to be hypoautofluorescent and well delineated, with foveal sparing atrophy in 10 eyes (71%) at baseline and in 6 eyes (42%) at the end of the follow-up. Some smaller atrophic areas were also present close to the central atrophy.

By comparing the multimodal imaging acquired at the baseline and the last follow-up visit of our patients' cohort, we detected remarkable progression of the atrophic process, involving both macula and peripheral posterior pole regions (Fig. 3). Structural OCT documented the progression of atrophy. SD-OCT assessment of central atrophy at baseline and follow-up revealed the number of eyes with cRORA, iRORA, and iORA stages (Table 1).[5] Pseudodrusen appeared as diffuse thickening above the RPE.

OCTA showed an almost preserved SCP in all zones, when compared with controls, with extension of CC impairment and less evident changes of DCP, mainly related to an already diffuse involvement at baseline (Fig. 3).

On the other hand, VD analyses in both DCP and CC showed significant alterations. All data are shown in Table 2. Remarkably, DCP and CC were unaltered only in preserved retinal zones with respect to controls. Analysis of the optic nerve head showed no significant differences between patients and controls except in the nerve choriocapillaris (nCC). BCVA severity was not related to nCC rarefaction.

Discussion

EMAP is differentiated from AMD on the basis of its development at a younger age and its symmetric involvement of both eyes. A progressive night blindness is followed by a rapid loss of central vision, leaving EMAP patients legally blind within only a few years.[7]

In AMD, pseudodrusen can be present in the subretinal space or between the RPE–photoreceptor layer; however, in EMAP, the pseudodrusen phenotype is characterized by diffuse subretinal thickening that is not limited to the posterior pole but also involves the mid-periphery.[7–9] A different inflammatory reaction in EMAP patients, as documented in other studies, could be a leading factor of faster disease progression and pseudodrusen formation. Moreover, an association between pseudodrusen and decreased choroidal thickness has been documented, suggesting that blood flow impairment also occurs in this disease.[7,10,11]

In the present study, we reported an extensive involvement of retinal vascular network in EMAP patients, detected by means of OCTA. In particular, SCP showed unremarkable alterations, whereas DCP and CC were strongly involved. It is worth

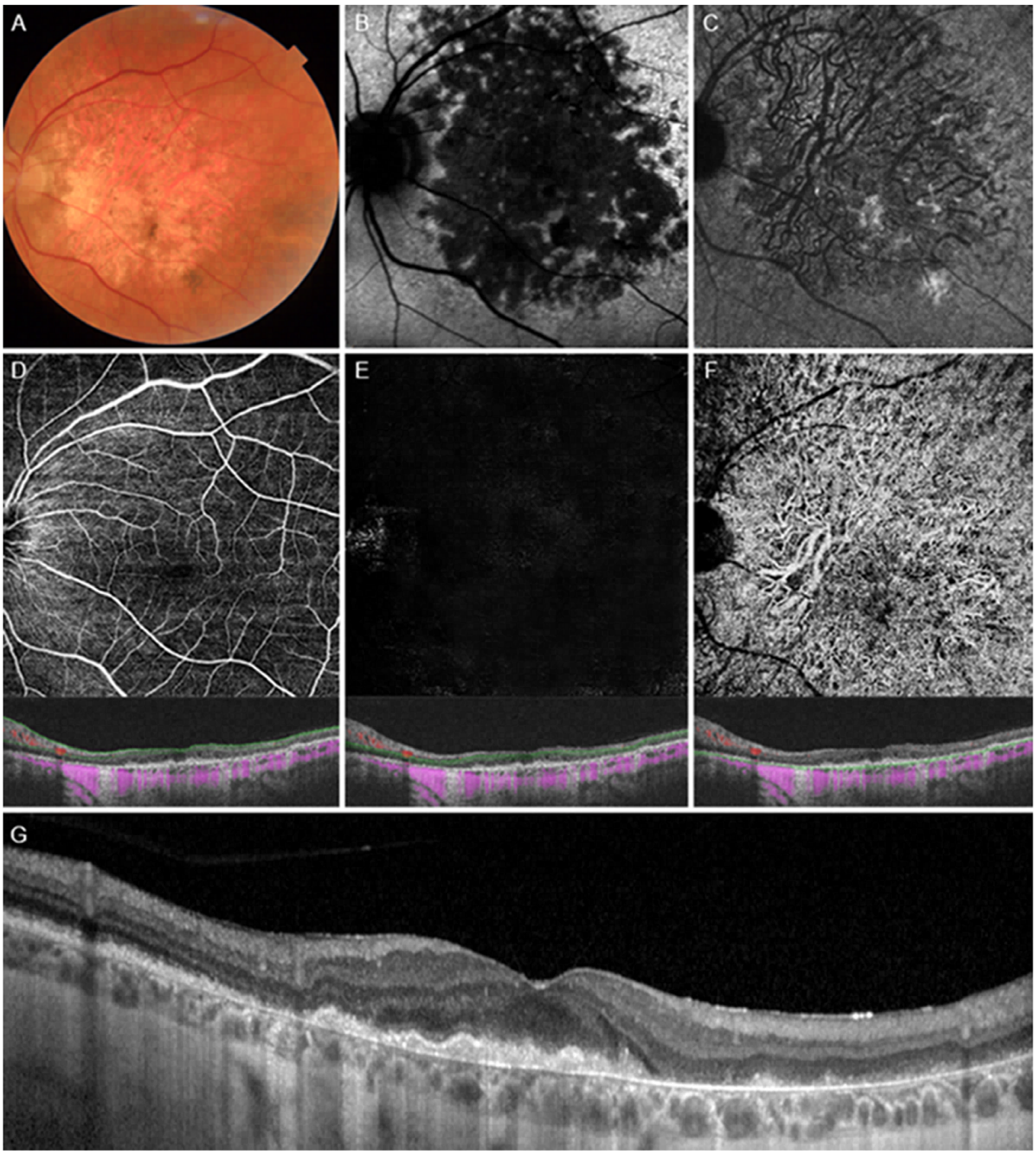

Figure 2. Multimodal retinal imaging of EMAP. (A) Fundus color photography shows atrophic zones extending vertically to the vascular arcades and the presence of small zones of pigmented alterations. (B) Fundus autofluorescence shows posterior pole hypoautofluorescence surrounded by a hyperautofluorescent margin. (C) Infrared autofluorescence reveals larger choroidal vessels through an atrophic retina. OCTA reconstructions of the retinal vascular network show (D) preserved superficial capillary plexus and (E) strongly altered deep capillary plexus and (F) choriocapillaris. (G) SD-OCT shows extensive loss of the outer retinal layers with a prominent barcode effect and thinned choroid.

noting the different behavior of DCP and CC alterations when comparing retinal zones A and B with respect to the corresponding regions in control eyes. DCP was not significantly altered in preserved retina compared with controls, and it showed no significant difference between junctional and atrophic zones. In contrast, CC was normal in the preserved retina but showed statistically significant differences among all of the analyzed subregions (preserved vs. junctional vs. atrophy). This means that DCP changes occur earlier

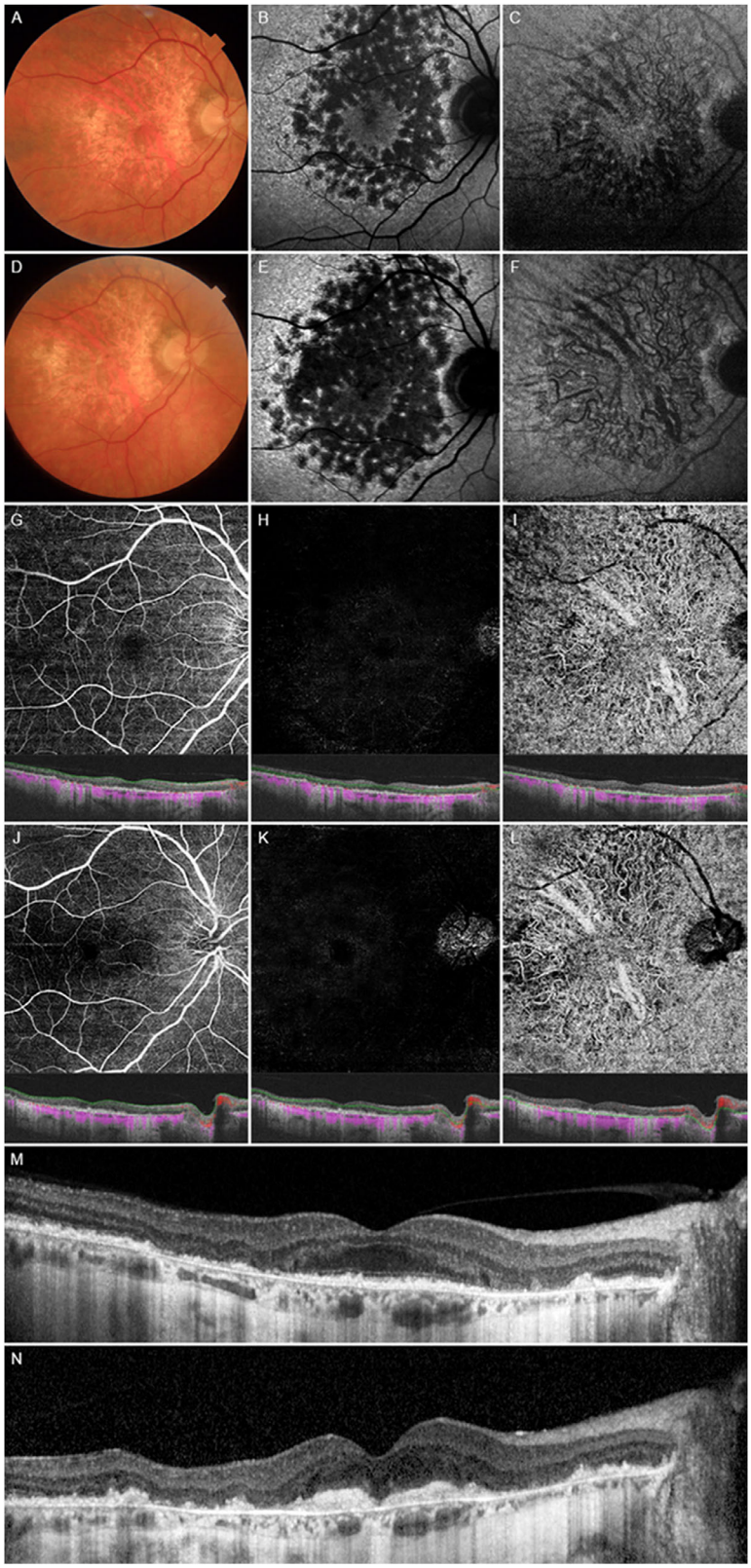

Figure 3. Progression of retinal changes over the follow-up. Color photography, fundus autofluorescence, and infrared autofluorescence clearly show the atrophic progression from baseline (A–C, respectively) to the last follow-up (D–F, respectively), oriented both vertically and close to the macular region. OCTA documents a still-preserved SCP (G and J) and further worsening of the DCP (H, K) and CC (I, L). Structural OCT shows the increased barcode effect at the follow-up, secondary to further loss of the RPE/photoreceptors complex, together with further retinal thinning (M, N).

Table 2. Correlation Analyses among OCTA Parameters

	Quantitative OCTA Analysis							
	SCP		DCP		CC			
Measure in Macula	Mean	SD	Mean	SD	Mean	SD		
EMAP preserved retina	0.41	0.03	0.42	0.03	0.50	0.01		
EMAP junctional zone	0.41	0.04	0.38	0.05	0.48	0.01		
EMAP atrophic retina	0.39	0.03	0.37	0.04	0.47	0.01		
Controls	0.41	0.01	0.43	0.01	0.50	0.01		
	nSCP		nDCP		nCC		RCP	
Measures in optic nerve	Mean	SD	Mean	SD	Mean	SD	Mean	SD
EMAP	0.35	0.04	0.44	0.05	0.49	0.02	0.4757	0.02
Controls	0.34	0.01	0.44	0.02	0.51	0.02	0.462	0.03
t-Test macula	SCP		DCP		CC			
Preserved retina vs. controls	>0.05		>0.05		>0.05			
Preserved retina vs. junctional zone	>0.05		**<0.01**		**<0.01**			
Preserved retina vs. atrophic retina	>0.05		**<0.01**		**<0.01**			
Junctional zone vs. controls	>0.05		**<0.01**		**<0.01**			
Junctional zone vs. atrophic retina	>0.05		>0.05		**<0.01**			
Atrophic retina vs. controls	>0.05		**<0.01**		**<0.01**			
t-Test optic nerve	nSCP		nDCP		nCC		RPC	
EMAP vs. controls	>0.05		>0.05		**<0.01**		>0.05	

Bold numbers indicate statistically significant data. nSCP, nerve superficial capillary plexus; nDCP, nerve deep capillary plexus; nCC, nerve choriocapillaris.

in EMAP and are almost the same in the junctional zone when compared with the atrophic retina. On the other hand, CC changes seemed to be more progressive, resulting in a consequential loss of integrity from the preserved retina to the junctional zone and up to the atrophic area. The non-significant changes in VD based on Optic Nerve head (ON) analysis and the absence of correlation between nCC rarefaction and the severity of visual acuity suggest that the pathology is primarily macular and without ON involvement.

Our results regarding the SCP can be considered somehow expected, as EMAP is considered to be an outer retinal pathology, leading to inner retinal alterations only in secondary stages. Furthermore, the finding of an earlier, stronger impairment of DCP is supported by the evidence of a greater sensitivity of this plexus to blood flow changes compared with SCP and CC.[12,13] Indeed, the progressive loss of RPE cells leads to downregulation of the trophic factors necessary to maintain retinal vascular integrity, causing increased distress to the DCP and CC with consequent perfusion loss.

We acknowledge that the present study has many limitations, especially bearing in mind the limited number of patients, the short and uneven follow-up, and the technical limitations typical of OCT and OCTA.[14]

Nevertheless, our study can serve as a pilot study to pave the road to further investigations attempting to better characterize a rare disease. Our pilot study found three different retinal regions in EMAP disease, as characterized by OCTA, corresponding to progressively deeper perfusion defects. Future studies are warranted to correlate the degree of DCP damage and the extent of atrophy.

Acknowledgments

Disclosure: **F. Rajabian**, None; **A. Arrigo**, None; **A. Bordato**, None; **S. Mercuri**, None; **F. Bandello**, None; **M. Battaglia Parodi**, None

References

1. Hamel CP, Meunier I, Arndt C, et al. Extensive macular atrophy with pseudodrusen-like

appearance: a new clinical entity. *Am J Ophthalmol*. 2009;147:609620.
2. Kamami-Levy C, Querques G, Rostaqui O, Blanco-Garavito R, Souied EH. Choroidal neovascularization associated with extensive macular atrophy with pseudodrusen-like appearance. *J Fr Ophtalmol*. 2014;37:780–786.
3. Battaglia Parodi M, Querques G. Choroidal neovascularization associated with extensive macular atrophy and pseudodrusen. *Optom Vis Sci*. 2015;92:S51–S54.
4. Kovach JL. Extensive macular atrophy with pseudodrusen imaged with OCT angiography. *Case Rep Ophthalmol Med*. 2018;2018: 8213097.
5. Sadda SR, Guymer R, Holz FG, et al. Consensus definition for atrophy associated with age-related macular degeneration on OCT: classification of atrophy report 3. *Ophthalmology*. 2018;125:537–548.
6. Al-Sheikh M, Ghasemi Falavarjani K, Akil H, Sadda SR. Impact of image quality on OCT angiography based quantitative measurements. *Int J Retina Vitreous*. 2017;3:13.
7. Douillard A, Picot MD, Delcourt C, et al. Dietary, environmental, and genetic risk factors of extensive macular atrophy with pseudodrusen, a severe bilateral atrophy of middle-aged patients. *Sci Rep*. 2018;8:6840.
8. Zweifel SA, Imamura Y, Spaide TC, Fujiwara T, Spaide RF. Prevalence and significance of subretinal drusenoid deposits (reticular pseudodrusen) in age-related macular degeneration. *Ophthalmology*. 2010;117:1775–1781.
9. Kovach JL, Schwartz SG, Agarwal A, et al. The relationship between reticular pseudodrusen and severity of AMD. *Ophthalmology*. 2016;123:921–923.
10. Smailhodzic D, Klaver CCW, Klevering BJ, et al. Risk alleles in CFH and ARMS2 are independently associated with systemic complement activation in age-related macular degeneration. *Ophthalmology*. 2012;119:339–346.
11. Scholl HPN, Fleckenstein M, Fritsche LG, et al. CFH, C3 and ARMS2 are significant risk loci for susceptibility but not for disease progression of geographic atrophy due to AMD. *PLoS ONE*. 2009;4:e7418.
12. Fawzi AA, Pappuru RR, Sarraf D, et al. Acute macular neuroretinopathy: long-term insights revealed by multimodal imaging. *Retina*. 2012;32:1500–1513.
13. Munk MR, Jampol LM, Cunha Souza E, et al. New associations of classic acute macular neuroretinopathy. *Br J Ophthalmol*. 2016;100:389–394.
14. Spaide RF, Fujimoto JG, Waheed NK, Sadda SR, Staurenghi G. Optical coherence tomography angiography. *Prog Retin Eye Res*. 2018;64:1–55.